Zhou *et al. Green Manuf Open* 2024;2:11
DOI: 10.20517/gmo.2024.032701

Green Manufacturing Open

Research Article

Open Access

Effect of low-energy laser peening on properties of NiCrBSi-WC/Co coating

Longlong Zhou[1,2], Weiling Guo[2], Hefa Zhu[3], Xiaohong Liu[1], Xinyuan Zhou[2], Zhenbing Cai[1], Zhiguo Xing[2]

[1]Tribology Research Institute, Key Lab of Advanced Technologies of Materials, Southwest Jiaotong University, Chengdu 610031, Sichuan, China.
[2]National Key Lab for Remanufacturing, Army Academy of Armored Forces, Beijing 100072, China.
[3]School of Materials Science and Engineering, Shanghai University, Shanghai 200444, China.

Correspondence to: Prof. Zhenbing Cai, Tribology Research Institute, Key Lab of Advanced Technologies of Materials, Southwest Jiaotong University, NO. 111, Section 1 North of Second Ring Road, Jinniu District, Chengdu 610031, Sichuan, China. E-mail: czb-jiaoda@126.com; Prof. Zhiguo Xing, National Key Lab for Remanufacturing, Army Academy of Armored Forces, 21 Dujiakan, Fengtai District, Beijing 100072, China. E-mail: xingzg2011@163.com

How to cite this article: Zhou L, Guo W, Zhu H, Liu X, Zhou X, Cai Z, Xing Z. Effect of low-energy laser peening on properties of NiCrBSi-WC/Co coating. *Green Manuf Open* 2024;2:11. https://dx.doi.org/10.20517/gmo.2024.032701

Received: 27 Mar 2024 **First Decision:** 22 May 2024 **Revised:** 9 Jun 2024 **Accepted:** 21 Jun 2024 **Published:** 3 Jul 2024

Academic Editors: Hong-Chao Zhang, Zhichao Liu **Copy Editor:** Pei-Yun Wang **Production Editor:** Pei-Yun Wang

Abstract

Low-energy laser peening (LE-LP) is a green and pollution-free surface deformation strengthening technology. In this work, LE-LP was used to improve the properties of NiCrBSi-WC/Co (Ni-WC) coating. The investigation focused on the impact of LE-LP on the coating microstructure, microhardness, residual stress, and tribological properties. The results showed that although laser hot melting damaged the coating surface, the phase structure of the coatings did not change significantly. The coating's hardness increased yet its surface roughness decreased as a result of the laser peening. Concurrently, after the LE-LP treatment, a residual compressive stress with an average value of -236 MPa was tested on the surface of the coatings. The average wear volume of the coating was reduced from 11.64 × 10^{-2} to 6.9 × 10^{-2} mm^3, and the average wear rate was reduced from 4.31 × 10^{-5} to 2.55 × 10^{-5}/N·mm^3.

Keywords: NiCrBSi-WC/Co coating, low-energy laser peening, microstructure, mechanical properties, tribological properties

INTRODUCTION

Wear failures are generated by the surface of the part[1,2]. Wear-resistant coatings prepared by supersonic

plasma spraying can improve the wear resistance of components[3,4]. NiCrBSi-WC/Co (Ni-WC) coating is widely used in aerospace and marine areas due to its excellent mechanical property and wear resistance[5,6]. The enhancement of coating properties has been a hot research topic[7,8].

Heat treatment is a traditional post-treatment method to improve coating properties and eliminate residual stress[9,10]. Compared with traditional heat treatment, surface deformation strengthening has the advantages of low impact on the substrate and introduction of residual compressive stresses on the surface[11,12]. It is an important technology to improve the wear resistance of components[13-16]. With the development of technology, surface deformation strengthening technology is gradually combined with coating's preparation to improve the properties of coatings[17,18].

Currently, The most widely used surface deformation peening techniques are shot peening, ultrasonic surface rolling and laser peening (LP)[19-21]. The characteristics of the coating are affected differently by different surface deformation peening methods. Li *et al.* shot-peened the Cr_3C_2-Al_2O_3-NiCr coatings and found that the surface microhardness of the coatings increased by 2.9 times[22]. The residual stress on the surface of the coating is -137 ± 7 MPa. And the wear rate of the coating is reduced by 98.7%. Zhao *et al.* used high temperature-assisted ultrasonic surface rolling to post-treat Ni-WC coating[23]. It is found that the surface roughness of the coating decreased by 49.04%, the surface microhardness of the coating increased by 38.4%, the surface stress changed from tensile stress to compressive stress, and wear amount reduced by 64.23%. Liu *et al.* found that LP increased the surface microhardness of NiCrBSi clad layers by 40.21%[24]. The surface residual compressive stresses were as high as -538 MPa. However, the surface roughness of the molten layer increased. In summary, it is feasible to use surface deformation strengthening techniques to improve the surface integrity of coatings. LP affects the coating to a depth of up to 2 mm and does not touch the coating, among other advantages[25].

Since the Ni-WC coatings prepared by supersonic plasma spraying have a laminar structure with internal defects such as pores and cracks, the Ni-WC coatings are prone to coating delamination and flaking during friction, so it is necessary to carry out post-treatment to improve the wear resistance of the coatings[26,27]. High-energy LP used energy of about 20 J/pulse and spot sizes fo about 3 to 5 mm. Low-energy LP (LE-LP) uses laser energy about 20 times smaller and a spot size of about 10 times smaller. Meanwhile, high-energy LP affects the metal to a depth of about 2 mm, and LE-LP affects it to a depth of about 100-200 μm. Compared to LP, the absorption layer is removed[1]. It saves costs and allows continuous work underwater[28,29]. Trdan *et al.* found that LE-LP increased the hardness of 6082-T651 Al alloy from 92 to 112 $HV_{0.2}$[30]. Residual surface compressive stresses up to -407 MPa were observed. Praveenkumar *et al.* found that the wear volume of TC4 alloy was reduced from 6.75 to 4.75 after LE-LP treatment[31]. LE-LP improves the mechanical properties and wear resistance of metals. On the other hand, LE-LP may cause the metal to heat up and develop holes and fissures in its surface[32,33]. At present, this technology is mainly used to improve the properties of bulk metal[34,35]. It not only enhances the properties of the metal but also has no effect on its phase structure. Therefore, the effects of LE-LP on the microstructure and properties of Ni-WC coatings need to be investigated.

In this work, we prepared Ni-WC coatings for the first time by supersonic plasma spraying technique. In order to improve the properties of the coatings, LE-LP was used. The effect of LE-LP on the microstructure and properties of the coatings was investigated.

METHODS

Powders

The raw material Ni-WC powder developed by Beijing Ryubon New Material Technology Co., Ltd. was used. Figure 1 shows the microstructure and chemical composition of two powders. NiCrBSi powder was prepared by atomized granulation, and hard ceramic WC/Co powder was sintered using 88 wt.% WC and 12 wt.% Co. Ni-WC powder was then prepared by mixing 10% WC/Co with 90% NiCrBSi. As seen in Figure 1, the distribution of NiCrBSi powder particle size is around 40-80 μm, while that of WC powder particle size is around 25 μm. The mass ratio of chemical composition elements of the two powders was analyzed by energy dispersive spectroscopy (EDS).

Coating preparation

Ni-WC coatings were prepared on 45 steel (medium carbon steel) substrates by using an efficient supersonic plasma spraying. The sample size was 10 mm × 10 mm × 10 mm. The substrates were ultrasonically cleaned and sandblasted before spraying. The surface of the substrate was free of impurities and maintained a certain roughness. Figure 2A shows the schematic diagram of the supersonic plasma sprayed Ni-WC coating. After the coating preparation, the coating was strengthened with LE-LP. The schematic diagram of LE-LP is shown in Figure 2B. The parameters of the sprayed and LE-LP prepared coatings are shown in Table 1. Laser energy was 100 mJ, with a pulse width of 10 ns and a spot diameter of 0.4 mm. The power density was 7.96 GW·cm^{-2}, and the repetition rate was 500 Hz. The wavelength was 532 ns, and the overlap rate was 50%. The confining layer was water.

Microstructure characterization

The three-dimensional (3D) morphology of the coatings was analyzed by using a white light interferometer (WLI) (SuperView W1, Chotest, China). The average value of a 1 mm^2 region chosen from three distinct coating locations was used to calculate the coating surface roughness. The surface and cross-section micro-morphology and elemental distribution of the coatings before and after LP were investigated using a scanning electron microscope (Hitachi SU8020, Japan) equipped with an energy spectrometer. The phase structure of the coatings was characterized using an X-ray diffractometer (XRD) (D8 Advance, Bruker, Germany). The Co target method was used to measure the XRD. The scanning rate is 4 °/min, and the wavelength is 0.17902 nm.

Mechanical properties characterization

The microhardness of the substrate and coating was tested using a microindenter (000 ZB, KELETI, China) after mechanical polishing treatment of the coating section. The residual stresses of the coatings were characterized by using an X-ray stress tester (XL-640, ST, China). The Co target method was used to measure the residual stresses.

Tribological properties

A multifunctional wear test equipment was used to perform reciprocating wear tests on the samples. Before the experiment, the coated samples and the pairs of body materials were ultrasonically cleaned. ZrO_2 was used for the test, and its specifications were 6 mm in diameter, 50 N load, 3 mm reciprocating distance, 5 Hz frequency, and 30 min duration.

RESULTS

Microstructure

The 3D morphologies before and after LE-LP treatment are displayed in Figure 3. The average surface roughness of the untreated coating is 18.389 μm; after LE-LP treatment, it is 16.924 μm [Figure 3]. This is due to the further compaction of the coating surface by the pulse-induced laser wave. Under the heat effect

Table 1. Coating preparation parameters

Parameters of spraying		Parameters of LE-LP	
H_2 gas flow	16 L/min	Laser energy	100 mJ
Ar gas flow	150 L/min	Pulse duration	10 ns
Powder feed rate	40 g/min	Spot diameter	0.4 mm
Spraying voltage	120 V	Power density	7.96 GW·cm^{-2}
Spraying current	460 A	Repetition rate	500 Hz
Spraying distance	130 mm	Wavelength	532 ns
Scanning velocity	4,000 mm/min	Overlap rate	50%
		Confining layer	Water

LE-LP: Low-energy laser peening.

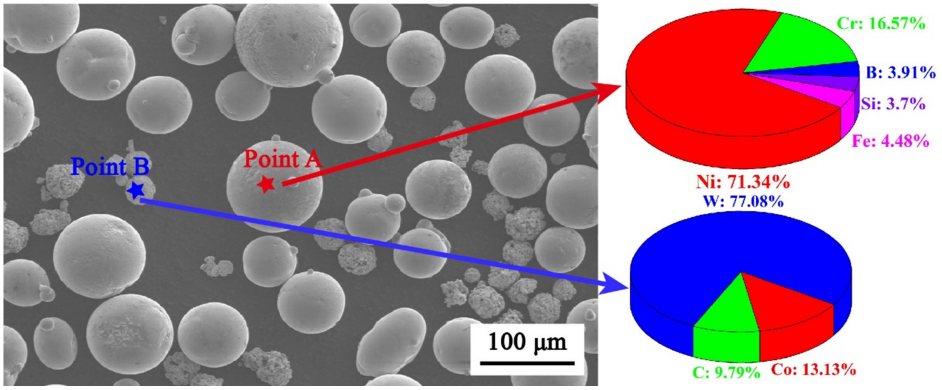

Figure 1. Particle size analysis and chemical composition of two powders.

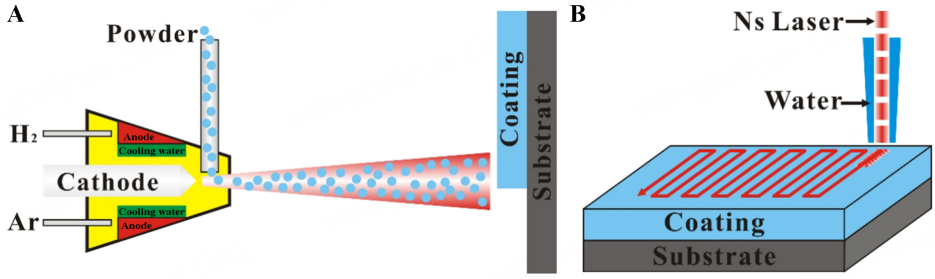

Figure 2. Coating preparation diagram. (A) Supersonic plasma spraying diagram; (B) LE-LP diagram. LE-LP: Low-energy laser peening.

of the LE-LP, the coating surface roughness was also further reduced. Ultimately, a synergistic effect between the heat influence and laser beam reduced the roughness.

In order to understand the thermal effects of the laser on the surface of the coating, the surface shape has been investigated. Figure 4 shows the microscopic morphology of the coating surface before and after LE-LP treatment. The untreated coating still has some unmelted particles and a comparatively smooth sprayed surface. Due to the lack of protection of the ablative layer during LE-LP treatment, the coating surface was inevitably subjected to thermal effects, and a large number of ablation holes could be observed on it. The reduction of surface roughness is caused by the secondary ablation of the unmelted particles. As can be seen from the pie chart in Figure 4, the mass percentage of O element increases from 1.04% to 2.70%. The results showed that the absence of the ablative layer led to an oxidation reaction on the coating surface, generating an oxide layer.

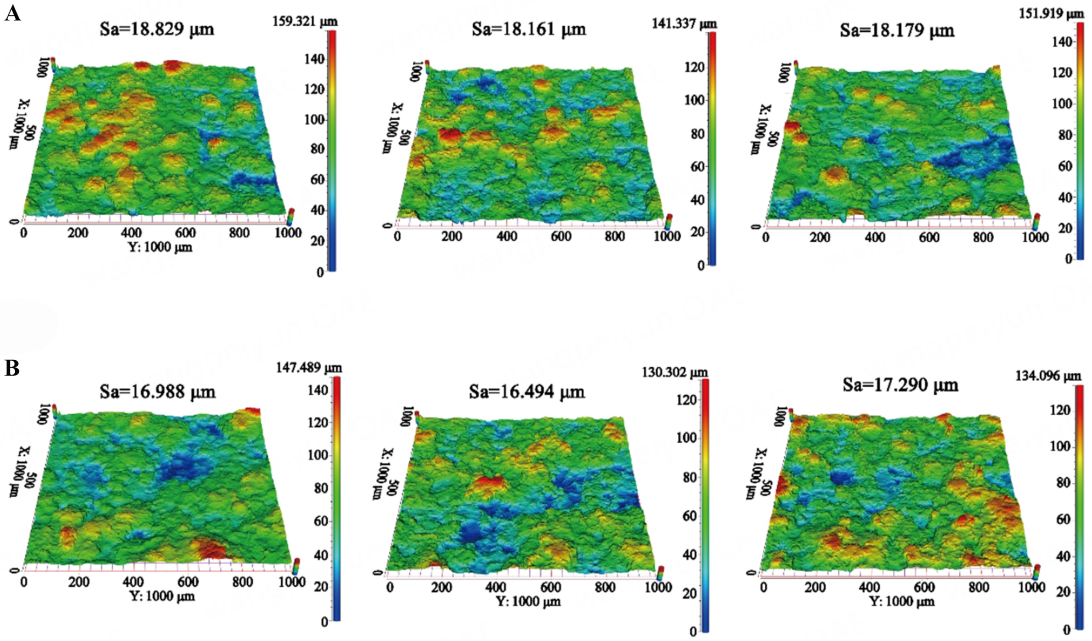

Figure 3. 3D morphology of the coating surface before and after LE-LP treatment. (A) 3D morphology and roughness of untreated coating surface; (B) 3D morphology and roughness of LE-LP treated coating. 3D: Three-dimensional; LE-LP: low-energy laser peening.

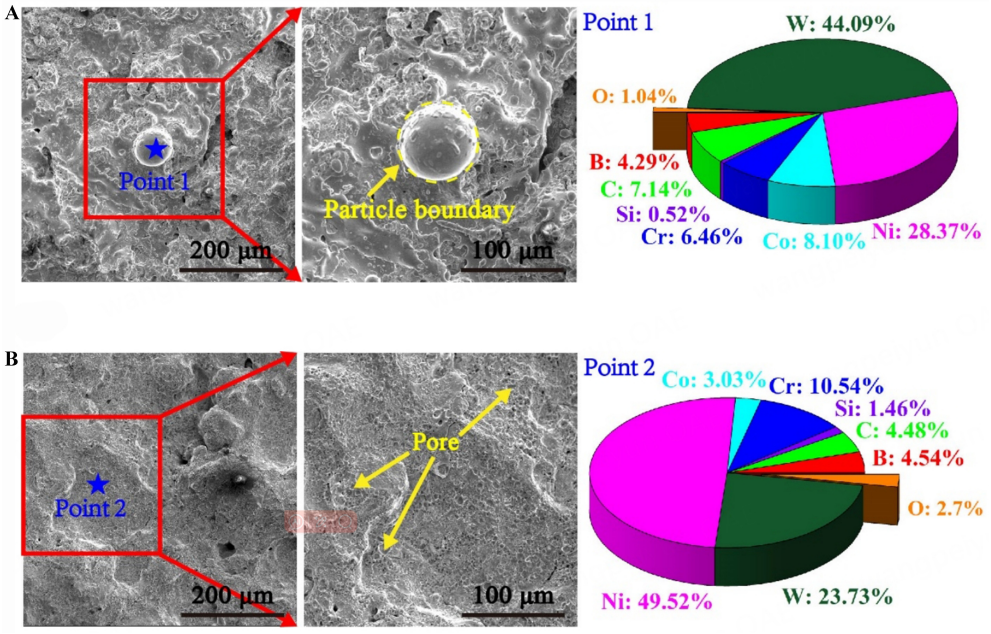

Figure 4. Surface morphology and EDS of coating surface before and after LE-LP treatment. (A) Surface morphology and EDS of untreated coating; (B) Surface morphology and elemental composition of LE-LP treated coating. EDS: Energy dispersive spectroscopy; LE-LP: low-energy laser peening.

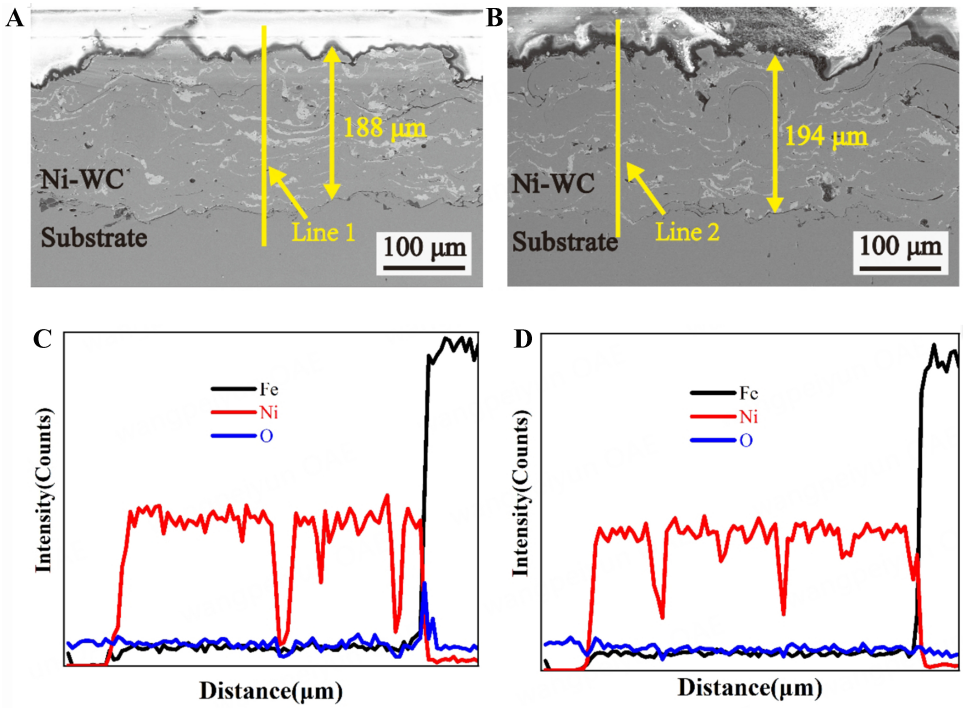

Figure 5. Cross-sectional morphology and EDS of coating before and after LE-LP treatment. (A) Cross-sectional morphology of untreated coating; (B) Cross-sectional morphology of LE-LP treated coating; (C) Distribution of elements of line 1; (D) Distribution of elements of line 2. EDS: Energy dispersive spectroscopy; LE-LP: low-energy laser peening.

Figure 5 shows the cross-sectional morphology and EDS of the coating both before and after LE-LP treatment. As shown in Figure 5, the cross-sectional morphology shows the laminar structure of thermal spraying. The ablation layer only occurs on the surface of the coating, and there is no ablative damage within the coating. Figure 5C and D shows the EDS of the coating cross-section elements. The EDS in the coating cross-sectional shows that there is no obvious mutation point of the O element in the coating. The O element is aggregated due to the presence of cracks at the interface. Combined with Figure 4, the ablation phenomenon only occurs on the surface of the coating and has no obvious effect on the inside of the coating.

Figure 6 shows the results of XRD pattern analysis of the coating surface. No noticeable additional diffraction peaks were observed on the coated surface following LE-LP treatment when compared to the XRD pattern of the untreated coating, indicating that the coating did not experience a noticeable phase shift following LE-LP. It is also further shown that the ablation damage of the laser on the coating occurs only on the surface of the coating.

Microhardness

LE-LP can cause elastic-plastic deformation of the material surface and improve the microhardness of the coating. The effect decreases as the depth increases. Figure 7 shows the microhardness of the coating cross-section. The hardness of the coating and the substrate was tested at 50 μm intervals using the bonding surface of the coating and the substrate as a standard reference. The average microhardness of the coating after LE-LP treatment increased from 713.8 to 799.9 $HV_{0.3}$ [Figure 7]. Furthermore, the hardness of the coating at 50 μm from the interface is around 720 $HV_{0.3}$, while the substrate's hardness is approximately 230 $HV_{0.3}$. It shows that the reinforced layer of the coating is approximately 140 μm thick following LE-LP treatment.

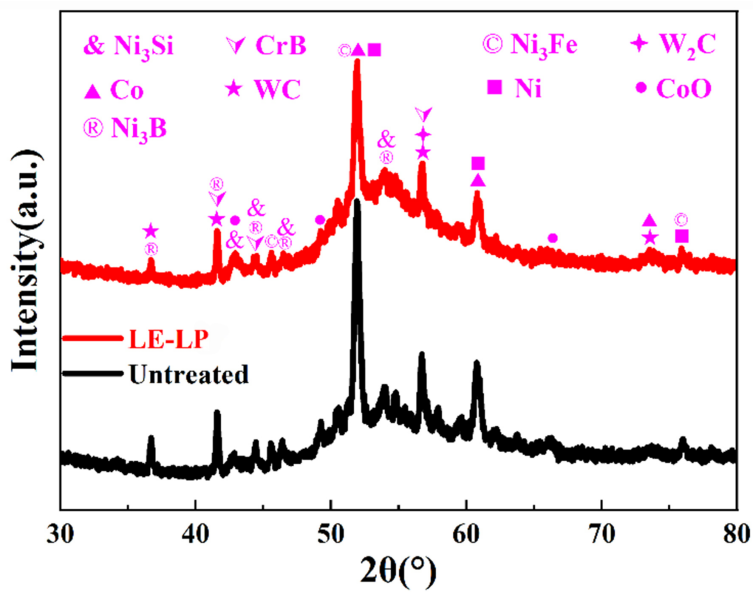

Figure 6. Effect of LE-LP treatment on XRD pattern of coating. LE-LP: Low-energy laser peening; XRD: X-ray diffractometer.

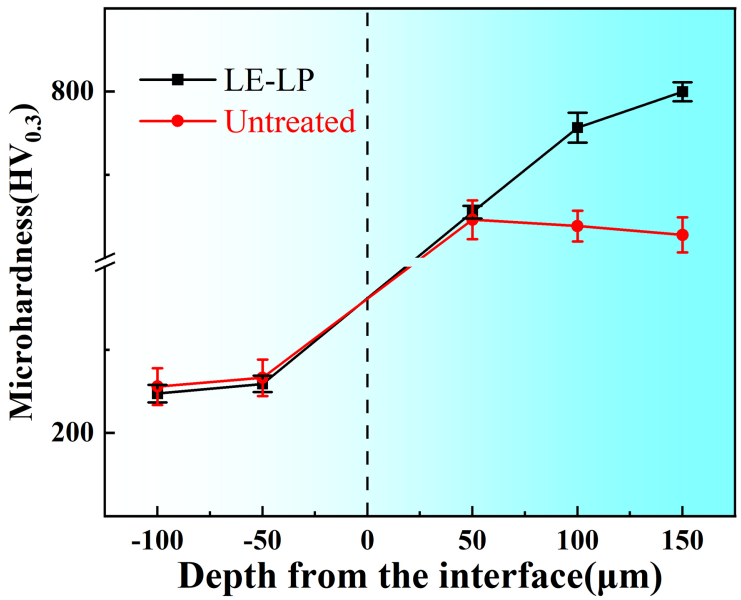

Figure 7. Microhardness of coating cross-section before and after LE-LP treatment. LE-LP: Low-energy laser peening.

Residual stress

Figure 8 displays the residual compressive stress on the coating surface before and after LE-LP. The average value of residual compressive stress on the surface of the untreated coating is -110 MPa, while after LE-LP treatment it is -236 MPa. Although the laser impact induces a thermal effect, the coating surface still undergoes plastic deformation and generates residual compressive stresses. The surface of the coating is subjected to the thermal effect of the laser, which, in general, causes residual tensile stresses on the surface of the material due to shrinkage after heating by laser irradiation. Nevertheless, there is still an improvement

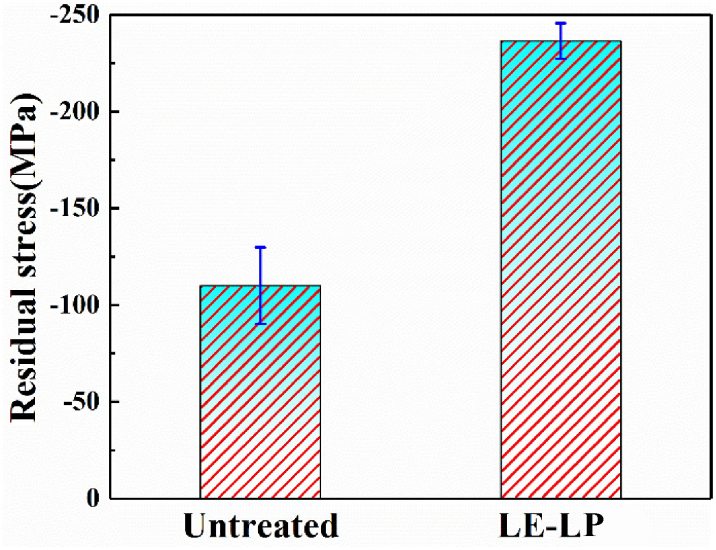

Figure 8. Residual stress on coating surface before and after LE-LP treatment. LE-LP: Low-energy laser peening.

in the residual compressive stress because of the overlap rate of the light spots, which cancels out the residual tensile stress areas by the residual compressive stress areas[36].

Tribological properties

The coefficient of friction of the Ni-WC coating is displayed in Figure 9 both before and after LE-LP treatment. Figure 9 shows that the coating wear may be separated into three primary stages: break-in, steady rising, and steady wear. It is also noted that the friction coefficients of the two coatings appear to have stabilized around 0.5.

Enhancing the microhardness and surface residual stress of coatings can increase their resistance to wear. Figure 10 demonstrates the tribological properties of Ni-WC coatings. After LE-LP treatment, the width of the front wear mark of coatings was reduced from 1,217.02 to 998.16 μm. The depth of the front wear mark of coatings was reduced from 72.39 to 55.76 μm. The average wear volume of the coating was reduced from 11.64×10^{-2} to 6.9×10^{-2} mm^3, and the average wear rate was reduced from 4.31×10^{-5} to 2.55×10^{-5}/N·mm^3. The wear resistance of the coating is enhanced by the increase in coating hardness and residual compressive stress following LE-LP treatment.

Figure 11 shows the morphology of the wear scar region before and after LE-LP treatment. An analysis of Figure 11 reveals the presence of visible plow furrows, localized spalling areas, and abrasive debris accumulation layers on the wear scar region. The wear mechanism is typical of abrasive wear. Combined with Figure 10, it can be seen that although LE-LP improved the wear resistance of the Ni-WC coating, it did not change the wear mechanism.

DISCUSSION

LE-LP is a surface deformation strengthening technology. Using plasma pressure and temperature generated by a pulsed laser, the metal surface undergoes plastic deformation, causing lattice dislocations, grain refinement, and so on. Residual compressive stresses are generated on the surface[37]. This improves the mechanical and tribological properties of the coating. Figure 12 shows a schematic diagram of the strengthening mechanism after LE-LP. LE-LP thermally affects the metal surface and reduces the roughness

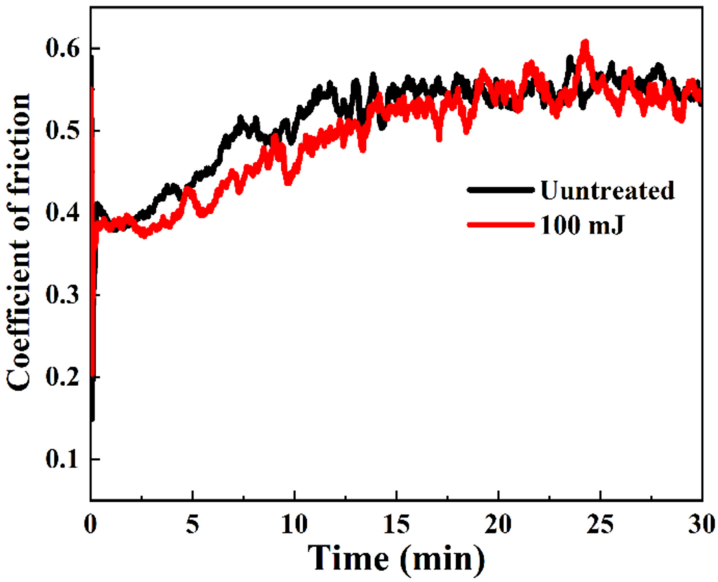

Figure 9. Coefficient of friction before and after LE-LP treatment. LE-LP: Low-energy laser peening.

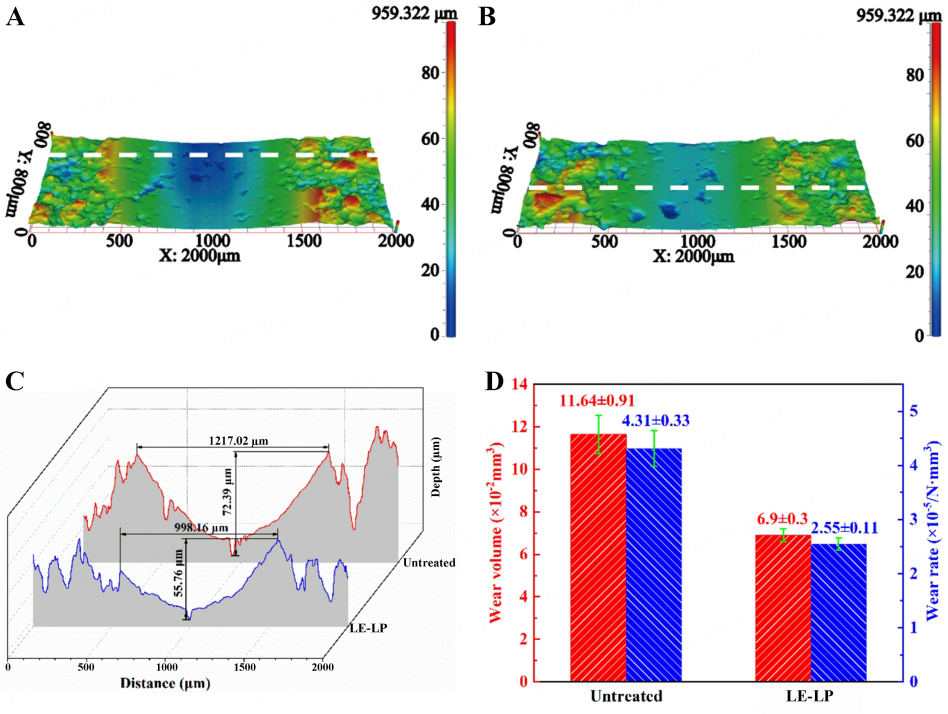

Figure 10. Wear performance of coating before and after LE-LP treatment. (A) Wear scar morphology of untreated coating; (B) Wear scar morphology of LE-LP treated coating; (C) Cross-sectional profile of wear scars; (D) Wear volume and rate. LE-LP: Low-energy laser peening.

of the coating surface through the synergistic effect of thermal effects and plastic deformation, and the results are shown in Figure 3. The technology thermally influences the coating surface [Figure 4] and produces a large number of ablative holes. Due to the high irradiance of the laser, the water is induced to decompose. Oxygen produced by water decomposition reacts with the ablative surface to form an oxide

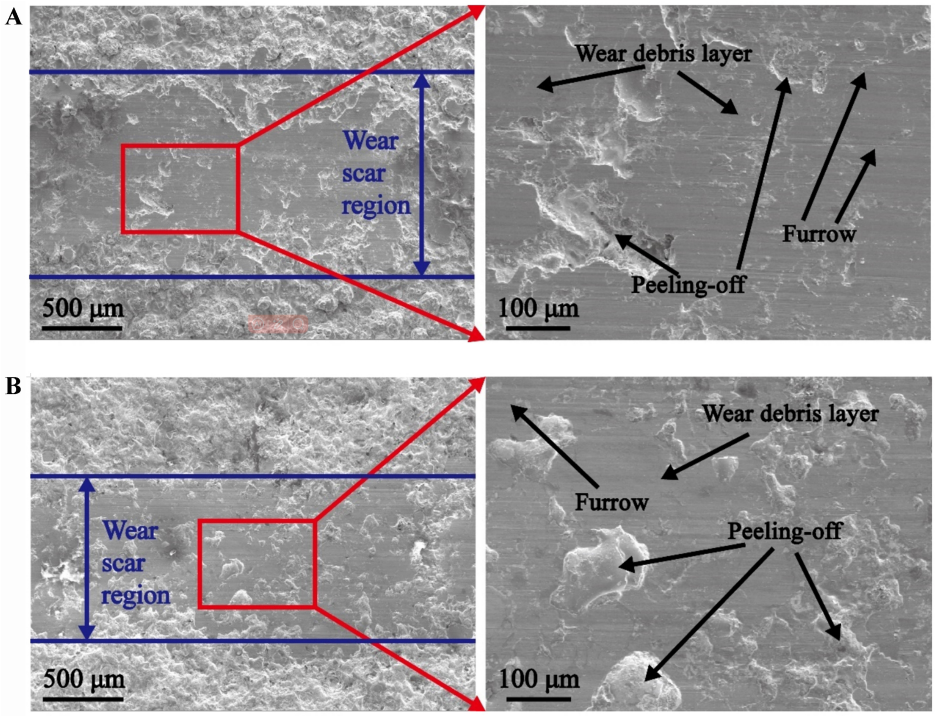

Figure 11. Morphology of wear scar region before and after LE-LP treatment. (A) Wear scar region of untreated; (B) Wear scar region of LE-LP treatment. LE-LP: Low-energy laser peening.

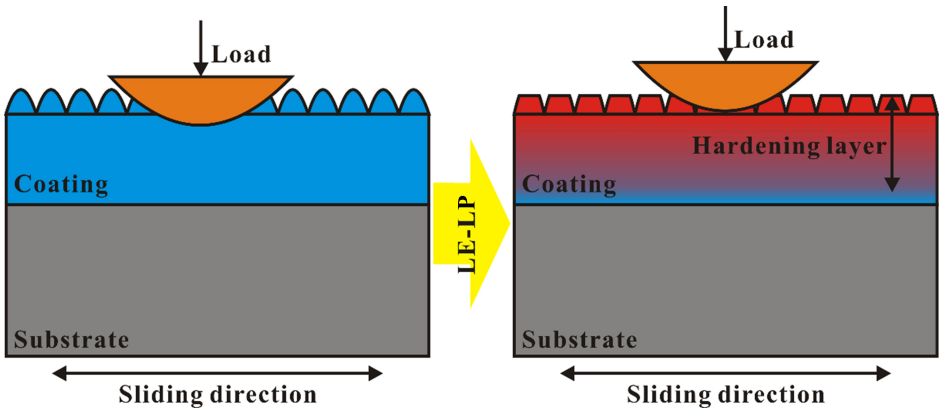

Figure 12. Schematic diagram of the strengthening mechanism after LE-LP. LE-LP: Low-energy laser peening.

layer[38]. However, the O elements produced due to ablation did not show significant oxidation characteristics at the coating cross section [Figure 5]. Combined with the XRD of the coating surface [Figure 6], it can be seen that the ablation effect of LE-LP on the coating occurs only on the coating surface. It shows that LE-LP on the coating not only retains the coating's phase structure, but also has a certain improvement effect on its surface roughness.

Table 2It is shown that the microhardness of the coating increases under the action of LE-LP [Figure 7], and the residual compressive stress on the coating surface improves [Figure 8], forming a hardened layer[39,40]. According to Archard's equation, the wear rate decreases with the increase of microhardness[22]. Meanwhile, the presence of the residual stress layer inhibits the generation and extension of wear cracks[41,42]. Coatings

Table 2. Effect of different surface deformation strengthening techniques on coatings

Technology	Coatings	Surface roughness	Microhardness	Residual stress	Tribological properties	Ref.
High-energy shot peening	Cr_3C_2-Al_2O_3-NiCr	/	From 497.3 to 674 HV	-131.7 MPa	Wear rate is reduced by 98.7%	[22]
Ultrasonic surface rolling	NiCrBSi + 15% WC	Reduced by 49.04%	From 631.4 to 873.9 $HV_{0.2}$	-404.2 MPa	Amount of wear reduced by 64.23%	[23]
LP	NiCrBSi	Increased by 530.7%	From 388 to 530 $HV_{0.2}$	-538 MPa	/	[24]
LE-LP	NiCrBSi + 10% WC	Reduced by 9.76%	From 704.3 to 797.8 $HV_{0.3}$	-236 MPa	Wear volume and wear rate were reduced by 40.72% and 40.83%	This work

LP: Laser peening; LE-LP: low-energy laser peening.

have a layered structure and are susceptible to delamination failure. During wear testing, interfacial cracks appearing on the subsurface can lead to delamination and severance of the upper layer. High residual compressive stress can retard the formation of microcracks[43,44]. The results of the wear performance of the coatings before and after LE-LP treatment are displayed in Figure 10, which makes it clear that the coating's wear resistance has greatly increased. The wear rate and wear volume of the coating are significantly reduced. The wear mechanism is abrasive wear. The work demonstrates that the wear resistance of Ni-WC coatings can be greatly increased using LE-LP, a surface deformation strengthening approach.

Table 2 shows the results of the surface deformation enhanced coating properties. It shows that different surface deformation peening techniques have distinct effects on the results of coating properties. High-Energy shot peening, ultrasonic surface tumbling and LE-LP decrease the surface roughness of the coating, while LP has the opposite effect. This is due to the fact that LP treats the laser-melted cladding layer, which has a low surface roughness. LP has a high irradiance, which produces tough nests on the surface of the coating after the impact, and, therefore, increases the surface roughness of the coating. The comparison also shows that the residual stresses are all manifested as residual compressive stresses. Although the range of coating hardness enhancement by LE-LP is significantly less than that of high-energy shot peening, ultrasonic surface tumbling and LP, there is an enhancement of coating wear resistance. Liu *et al.* found that the hardness and residual stress of the coatings were enhanced with the laser energy, but critical values existed[24]. LE-LP offers advantages such as a simple process, no contact, *etc.*

CONCLUSION

In this work, LE-LP was used to improve the properties of Ni-WC coatings. The effect of LE-LP on the microstructure, mechanical properties and wear resistance of the coatings was investigated. The following conclusions were drawn from the work.

(1) The surface roughness of the coating is reduced by a combination of plastic deformation and thermal influences. An oxidation reaction occurs on the surface of the coating, producing an oxide film.
(2) The microhardness of the coating increased from 704.3 to 797.8 after LE-LP treatment. The residual stress on the coating surface with an average value of -110 MPa was transformed into a residual stress with an average value of -236 MPa. A hardened layer of about 140 μm was formed.
(3) The wear resistance of the coating was further improved by LE-LP. The average wear volume of the coating was reduced from 11.64×10^{-2} to 6.9×10^{-2} mm^3, and the average wear rate was reduced from 4.31×10^{-5} to 2.55×10^{-5}/N·mm^3. The wear mechanism is abrasive wear.

LE-LP can improve the tribological properties of coatings. The research foundation for LE-LP to enhance tribological characteristics of coatings is supplied by this work. LE-LP is a post-processing method that can be combined with additive manufacturing.

DECLARATIONS

Author's contributions

Conceptualization: Zhou L, Xing Z
Formal analysis: Zhou L, Cai Z
Methodology: Zhou X, Zhu H
Data curation, writing - original draft: Zhou L
Writing - review and editing: Cai Z
Supervision: Guo W, Liu X

Availability of data and materials

Not applicable.

Financial support and sponsorship

The paper was financially supported by the General program of the National Natural Science Foundation of China (Grant No. 52275227), the National Key Research and Development Program of China (Grant 2022YFB3401901), Key Program of National Natural Science Foundation of China (Grant U2067221), Sichuan Provincial Science and Technology Program (Grants 2022JDJQ0019 and 2022ZYD0029) and Ship Vibration and Noise Key Laboratory Program (Grants 6142204210707 and JCKY2022207CI10).

Conflicts of interest

All authors declared that there are no conflicts of interest.

Ethical approval and consent to participate

Not applicable.

Consent for publication

Not applicable.

REFERENCES

1. Yu Y, Gong J, Fang X, et al. Comparison of surface integrity of GH4169 superalloy after high-energy, low-energy, and femtosecond laser shock peening. *Vacuum* 2023;208:111740. DOI
2. Cai Z, Li Z, Yin M, Zhu M, Zhou Z. A review of fretting study on nuclear power equipment. *Tribol Int* 2020;144:106095. DOI
3. Zhou L, Li X, He D, et al. Study on properties of potassium sodium niobate coating prepared by high efficiency supersonic plasma spraying. *Actuators* 2022;11:28. DOI
4. Wang J, Lu Z, Huang Y, et al. The mechanism for the enhanced mechanical and piezoelectricity properties of La_2O_3 doped $BaTiO_3$ ceramic coatings prepared by plasma spray. *J Alloys Compd* 2022;897:162944. DOI
5. Sha J, Chen L, Liu Y, et al. Phase transformation-induced improvement in hardness and high-temperature wear resistance of plasma-sprayed and remelted NiCrBSi/WC coatings. *Metals* 2020;10:1688. DOI
6. Rachidi R, El Kihel B, Delaunois F. Microstructure and mechanical characterization of NiCrBSi alloy and NiCrBSi-WC composite coatings produced by flame spraying. *Mater Sci Eng B* 2019;241:13-21. DOI
7. Zhou J, Huang Y, Cai Z, et al. Preparation of NiCrBSi-WC/Co coatings by stable magnetic field assisted supersonic plasma spraying and its wear resistance mechanism. *Mater Charact* 2022;194:112433. DOI
8. Zhou J, Guo W, He D, et al. Study on preparation and wear resistance of NiCrBSi-WC/Co composite coatings by pulsed magnetic field assisted supersonic plasma spraying. *Surf Coat Technol* 2022;448:128897. DOI

9. Li GJ, Li J, Luo X. Effects of high temperature treatment on microstructure and mechanical properties of laser-clad NiCrBSi/WC coatings on titanium alloy substrate. *Mater Charact* 2014;98:83-92. DOI
10. Liu L, Xu H, Xiao J, Wei X, Zhang G, Zhang C. Effect of heat treatment on structure and property evolutions of atmospheric plasma sprayed NiCrBSi coatings. *Surf Coat Technol* 2017;325:548-54. DOI
11. Liu W, Yang X, Wan Z, Xia G, Li D, Wang S. Surface strengthening technology for mechanical parts. *Surf Rev Lett* 2021;28:2030006. DOI
12. Li M, Liu D, Bai Z, et al. Hot salt corrosion behavior of Ti–6Al–4V alloy treated with different surface deformation strengthening processes. *Mater Chem Phys* 2023;309:128410. DOI
13. Yin M, Cai Z, Li Z, Zhou Z, Wang W, He W. Improving impact wear resistance of Ti-6Al-4V alloy treated by laser shock peening. *T Nonferr Metal Soc* 2019;29:1439-48. DOI
14. Li Z, Guo X, Yang Z, Cai Z, Jiao Y. Effect of ultrasonic surface rolling process on the microstructure and corrosion behavior of zirconium alloy in high-temperature water condition. *Mater Chem Phys* 2024;311:128546. DOI
15. Yin M, Cai Z, Zhang Z, Yue W. Effect of ultrasonic surface rolling process on impact-sliding wear behavior of the 690 alloy. *Tribol Int* 2020;147:105600. DOI
16. Olugbade TO, Lu J. Literature review on the mechanical properties of materials after surface mechanical attrition treatment (SMAT). *Nano Mater Sci* 2020;2:3-31. DOI
17. Yao H, Hu X, Yi Z, et al. Microstructure and improved anti-corrosion properties of cold-sprayed Zn coatings fabricated by post shot-peening process. *Surf Coat Technol* 2021;422:127557. DOI
18. Zhang Y, Li L, Wang X, et al. Experimental study on aluminum bronze coating fabricated by electro-spark deposition with subsequent ultrasonic surface rolling. *Surf Coat Technol* 2021;426:127772. DOI
19. Chen X, Xie X, Zhang Y, Wang H, Liang Z. Tungsten carbide coating prepared by ultrasonic shot peening to improve the wear properties of magnesium alloys. *J Mater Res Technol* 2023;26:2451-64. DOI
20. Cui Z, Qin Z, Dong P, Mi Y, Gong D, Li W. Microstructure and corrosion properties of FeCoNiCrMn high entropy alloy coatings prepared by high speed laser cladding and ultrasonic surface mechanical rolling treatment. *Mater Lett* 2020;259:126769. DOI
21. Lu JZ, Xue KN, Lu HF, Xing F, Luo KY. Laser shock wave-induced wear property improvement and formation mechanism of laser cladding Ni25 coating on H13 tool steel. *J Mater Process Tech* 2021;296:117202. DOI
22. Li F, Zhang C, Pang Q, Fang G, Xu G. Effect of high-energy shot peening on properties of high-velocity oxygen-fuel spraying. *Coatings* 2023;13:872. DOI
23. Zhao Y, He Y, Zhang J, Meng C, Zhang X, Zhang S. Effect of high temperature-assisted ultrasonic surface rolling on the friction and wear properties of a plasma sprayed Ni/WC coating on #45 steel substrate. *Surf Coat Technol* 2023;452:129049. DOI
24. Liu G, Xue W, Cao Y, et al. Influence of laser shock peening on microstructure and property of Ni60 cladding layer and the combined area of 20CrNiMo alloy. *J Laser Appl* 2023;35:022009. DOI
25. Lin Y, Cai Z, Li Z, et al. Study on the abrasive wear behavior of laser shock peening Ti-6Al-4V titanium alloy under controlled cycling impact. *Wear* 2019;426-7:112-21. DOI
26. Dong T, Zhou X, Li G, Liu L, Wang R. Microstructure and corrosive wear resistance of plasma sprayed Ni-based coatings after TIG remelting. *Mater Res Express* 2018;5:026411. DOI
27. Geng Z, Hou S, Shi G, Duan D, Li S. Tribological behaviour at various temperatures of WC-Co coatings prepared using different thermal spraying techniques. *Tribol Int* 2016;104:36-44. DOI
28. Fang X, Gong J, Yu Y, et al. Study on the fretting wear performance and mechanism of GH4169 superalloy after various laser shock peening treatments. *Opt Laser Technol* 2024;170:110301. DOI
29. Abeens M, Muruganandhan R, Thirumavalavan K. Effect of Low energy laser shock peening on plastic deformation, wettability and corrosion resistance of aluminum alloy 7075 T651. *Optik* 2020;219:165045. DOI
30. Trdan U, Porro JA, Ocaña JL, Grum J. Laser shock peening without absorbent coating (LSPwC) effect on 3D surface topography and mechanical properties of 6082-T651 Al alloy. *Surf Coat Technol* 2012;208:109-16. DOI
31. Praveenkumar K, Swaroop S, Manivasagam G. Effect of multiple laser shock peening without coating on residual stress distribution and high temperature dry sliding wear behaviour of Ti-6Al-4 V alloy. *Opt Laser Technol* 2023;164:109398. DOI
32. Wang H, Keller S, Chang Y, et al. Effect of laser shock peening without protective coating on the surface mechanical properties of NiTi alloy. *J Alloys Compd* 2022;896:163011. DOI
33. Petronić S, Čolić K, Đorđević B, Milovanović D, Burzić M, Vučetić F. Effect of laser shock peening with and without protective coating on the microstructure and mechanical properties of Ti-alloy. *Opt Laser Eng* 2020;129:106052. DOI
34. Yang Y, Zhou W, Guo Y, et al. Effect of laser shock peening without protective coating on surface integrity of titanium-based carbon-fibre/epoxy laminates. *Opt Laser Technol* 2023;167:109685. DOI
35. Park C, Jung D, Chun E, Ahn S, Jang H, Kim Y. Effect of laser shock peening without coating on fretting corrosion of copper contacts. *Appl Surf Sci* 2020;514:145917. DOI
36. Sano Y, Akita K, Sano T. A mechanism for inducing compressive residual stresses on a surface by laser peening without coating. *Metals* 2020;10:816. DOI
37. Sano Y. Quarter century development of laser peening without coating. *Metals* 2020;10:152. DOI
38. Xue D, Jiao Y, He W, Shen X, Gao Y, Wang L. Investigations into the improvement of the mechanical properties of Ti-5Al-4Mo-4Cr-2Sn-2Zr titanium alloy by using low energy laser peening without coating. *Materials* 2020;13:1398. DOI PubMed PMC

39. Wang H, Jürgensen J, Decker P, et al. Corrosion behavior of NiTi alloy subjected to femtosecond laser shock peening without protective coating in air environment. *Appl Surf Sci* 2020;501:144338. DOI
40. Jiao Y, He W, Shen X. Enhanced high cycle fatigue resistance of Ti-17 titanium alloy after multiple laser peening without coating. *Int J Adv Manuf Technol* 2019;104:1333-43. DOI
41. Troiani E, Zavatta N. The effect of laser peening without coating on the fatigue of a 6082-T6 aluminum alloy with a curved notch. *Metals* 2019;9:728. DOI
42. Chen Z, Wang Z, Liu J, et al. Enhancing the tribological properties of TA1 pure titanium by modulating the energy of pulsed laser nitriding. *Opt Laser Technol* 2024;169:110118. DOI
43. Cao Y, Sun J, Ma F, et al. Effect of the microstructure and residual stress on tribological behavior of induction hardened GCr15 steel. *Tribol Int* 2017;115:108-15. DOI
44. Guan J, Wang L, Mao Y, Shi X, Ma X, Hu B. A continuum damage mechanics based approach to damage evolution of M50 bearing steel considering residual stress induced by shot peening. *Tribol Int* 2018;126:218-28. DOI